European Polymer Journal 66 (2015) 458–469

Contents lists available at ScienceDirect

European Polymer Journal

journal homepage: www.elsevier.com/locate/europolj

The structural evolution of high-density polyethylene during crazing in liquid medium

Alena Yu. Yarysheva [a,*], Ekaterina G. Rukhlya [a], Larisa M. Yarysheva [a], Dmitry V. Bagrov [b,c], Aleksandr L. Volynskii [a], Nikolai F. Bakeev [a]

[a] Department of Chemistry, Lomonosov Moscow State University, Leninskie Gory 1-3, 119991 Moscow, Russia
[b] Department of Biology, Lomonosov Moscow State University, Leninskie Gory 1-3, 119991 Moscow, Russia
[c] SRI of Physical-Chemical Medicine, Malaya Pirogovskaya, 1a, 119435 Moscow, Russia

ARTICLE INFO

Article history:
Received 27 January 2015
Received in revised form 2 March 2015
Accepted 4 March 2015
Available online 19 March 2015

Keywords:
Crazing
HDPE structure
HDPE deformation
Semicrystalline polymers
Atomic force microscopy

ABSTRACT

Atomic force microscopy (AFM) was employed to study structural transformations occurring in high-density polyethylene (HDPE) during deformation in a liquid medium by crazing mechanism. Processing of the obtained images yielded the parameters of HDPE structure at different tensile strains. It was shown that crazing causes the development of a fibrillar–porous structure in the interlamellar space, the fragmentation of lamellae, and the displacement of lamella fragments relative to each other. Moreover, the deformation is accompanied by the separation of lamellae and the long period increases in the proportion to the tensile strain. The scheme of HDPE deformation upon crazing in liquid medium was constructed based on the AFM images.

1. Introduction

High-density polyethylene (HDPE) is a profoundly investigated semicrystalline polymer, and numerous works [1–10] have been focused on studying the mechanism of its deformation and the evolution of its structure upon stretching in air. At the same time, items made of HDPE are frequently exploited in contact with various liquid and gaseous media. In this situation, physically active media, such as hydrocarbons, oils, alcohols, and surfactants, which do not modify the chemical structure of the polymer, can affect the mechanical properties of polyethylene and decrease its endurance. Since the breakage of a polymer being deformed in a liquid medium is preceded by nucleation of crazes and cracks, the functional properties of polymers are estimated by monitoring their appearance upon the complex action of an ambient liquid and stress [11–16]. In the literature, this phenomenon is referred to as the environmental stress cracking/crazing (ESC), and the main efforts of researchers have been focused on the suppression or deceleration of the craze/crack development.

At the same time, the development of crazes upon polymer deformation in physically active media (wet crazing or solvent crazing) may be a positive factor, because this process is accompanied by the appearance of a finely disperse fibrillar–porous structure with pore and fibril sizes of about 5–20 nm [17–19]. Works [19–21] were the first to determine the conditions under which deformation of amorphous glassy and semicrystalline polymers in liquid media occurs by the crazing mechanism and gives rise to the formation of nanoporous materials with a porosity as high as 40–60%. It is of particular interest that polymer deformation in solutions of various low- and high-molecular-mass compounds is accompanied by their penetration into the nanoporous structure of crazes. Therefore, polymer crazing in liquid media may be considered as a

* Corresponding author.
E-mail address: alyonusha@gmail.com (A.Yu. Yarysheva).

http://dx.doi.org/10.1016/j.eurpolymj.2015.03.003
0014-3057/

method for obtaining nanoporous materials (membranes and sorbents) and as a process for producing nanocomposites and highly disperse polymer–polymer blends [22–28].

Hence, the study of polymer crazing in physically active media is an interesting problem from the viewpoints of both determining the influence of liquid media on the deformation mechanism of polymers and obtaining highly disperse fibrillar–porous structures in them.

Spherulites consist of lamellae, which are oriented in different directions, and form the morphology that prevails in crystalline structures of polymers that are produced by crystallization from melts in the absence of substantial external actions. Being crystallized under the conditions of a tensile stress, a melted polymer may form samples containing anisotropically arranged stacks of lamellae, which are predominantly oriented perpendicularly to an extrusion axis [29–37]. Such anisotropic structures, which are referred to as row-structures, are more convenient for investigating structural rearrangements that accompany the deformation of semicrystalline polymers, because these structures are characterized by a smaller number of possible orientations relative to an applied force. Therefore, the study of their structural transformations upon deformations directed along and normal to the extrusion axis makes it possible to simulate the deformation of the lamellar stacks occurring in the equatorial and meridional regions of the spherulites, respectively.

Fundamental data on the structural evolution of HDPE upon its stretching in air have been obtained by wide- and small-angle X-ray scattering [38,39], differential scanning calorimetry, IR [40] and Raman [41] spectroscopy, as well as atomic force [42,43] and electron microscopy [44–47]. It is obvious that microscopic investigations are of particular interest, because they enable one to directly observe structural transformations that result from polymer deformation.

Polymer deformation by the crazing mechanism in liquid media is accompanied by fibrillization of a polymer material and the development of a porous structure with a large surface area (as large as 100 m^2/g) [17,19]. As a result, the structure of crazed polymers is thermodynamically unstable and substantially changes after stress relaxation or removal of the medium. Therefore, the investigation of the structure of deformed polymers directly in a physically active media and under the conditions preventing them from shrinkage is of especial significance. As has been shown [48], atomic force microscopy (AFM) is very suitable for investigation of polymer deformed by the crazing mechanism, although this method allows one to examine only the surface of a polymer film. Note that the structure of HDPE deformed by the crazing mechanism was investigated by AFM in the same liquid medium in which the deformation had been carried out. Samples deformed to different tensile strains were fastened to a circular frame to prevent them from shrinkage. The samples thus prepared made it possible to observe the structure that directly resulted from the polymer stretching.

The goal of this work is the AFM investigation of the structural evolution of HDPE with an initial row-structure upon stretching in a liquid physically active medium to different tensile strains. The work consists of several sections. The initial HDPE structure is considered in the first section of the work, and the second section is devoted to the features of HDPE deformation in the liquid media and in air. Then, AFM is employed to characterize the structures of HDPE deformed in the liquid medium to different tensile strains.

2. Experimental

2.1. Materials

The objects for the study were HDPE (M_w = 210000 and M_n = 7000 g/mol) films 25 μm thick (Stamylan, DSM) produced by extrusion blow molding. Films with sizes of 40 × 20 mm were deformed upon planar stretching in a water–ethanol solution (1:7, vol/vol) at room temperature and a rate of 5.4 mm/min.

2.2. Methods

2.2.1. Differential scanning calorimetry (DSC) experiments

The experiments were performed using a TA 4000 thermoanalyzer (Metter). The mass of an examined sample was 1.5 mg. Ideal crystal melting heat, which was used to calculate the degree of crystallinity, was 293 J/g. The heating rate was 10 K/min. Lamella thickness was calculated by the following formula:

$$L_c = K_c L_{saxs}(d/d_c), \quad (1)$$

where L_{saxs} is the long period determined by small-angle X-ray scattering (25 nm); d and d_c are the densities of the polymer and its crystalline phase (0.960 and 1.003), respectively; and K_c is the degree of crystallinity (59%) determined from the DSC data.

2.2.2. X-ray diffraction analysis

Small- and wide-angle X-ray scattering measurements were carried out with a Nanostar instrument (Bruker AXS) equipped with a Cu Kα generator of X-rays (λ = 0.154 nm).

2.2.3. Volume strain

Volume strain (W) of the deformed polymer was calculated from changes in the geometric sizes of the films as the ratio of volume increment (ΔV) resulting from film stretching to initial sample volume (V_0), $W = (\Delta V/V_0) \times 100$ (%). The geometric dimensions of the deformed HDPE sample were measured with a projector with a tenfold magnification and an IZV2 optimeter, the measurement error was ±1 μm.

2.2.4. Procedure for investigating the structure of HDPE deformed in the liquid medium

The structure of HDPE was studied in the following way. Initially, a sample was stretched to some tensile strain with a stretching unit operating in the liquid medium. Then, without removing the sample from the liquid medium and the clamps of the stretching unit, it was fastened to a circular frame to fix its sizes throughout the perimeter

and prevent it from shrinkage. The frame with the sample was placed into a Petri dish filled with the medium (water–ethanol solution) in which the stretching had been implemented. A support was mounted under the center of the film to reduce vibration. This system enabled us to carry out the AFM examination of the deformed film surface in the presence of the liquid under the conditions that prevented the samples from shrinkage.

2.2.5. Atomic force microscopy experiments (AFM)

All AFM experiments were carried out using a Solver Pro-M atomic force microscope (NT-MDT, Russia, Zelenograd) in the "scanning by probe" configuration. A Smena scanning head equipped with closed-loop feedback sensors was used (scanner range of $100 \times 100 \times 7$ μm). The scanning was carried out in the contact and tapping modes. The scanning was performed using MSCT-AUHW cantilevers (Bruker, former Veeco, Santa Barbara, California, United States).

The AFM images were processes using the Femtoscan online software package (Advanced Technologies Center, Russia). Each scan was processed using "Fit Lines" and "Plane Fit" functions to avoid the shift of rows and the general slope, respectively. When necessary, the noise was reduced by median filtering or averaging. In some cases, the macroscopic height variations were removed using the spline filtering. When plotting and analyzing the sections, each section profile was constructed by averaging the profiles over three adjacent section lines.

3. Results and discussion

3.1. Structure of initial HDPE

The initial structure of HDPE selected for this work was studied by the wide (WAXS)- and small-angle X-ray scattering (SAXS), differential scanning calorimetry (DSC), scanning electron microscopy (SEM), and atomic force microscopy (AFM) [48]. According to the DSC data, the degree of crystallinity of HDPE films was 59%. HDPE films were prepared by extrusion blow molding, i.e., under the conditions of polymer crystallization in a stress field. Under these conditions, the films were formed at a high rate; therefore, melt macromolecules acquired extended conformations, and, initially, they crystallized to form fibrils in the film extrusion direction. These fibrils act as nuclei for the crystallization of the bulk. As the temperature was decreased, the crystallization process led to the formation of lamellae containing folded chains, the epitaxial growth of which proceeded perpendicularly to the direction of the melt flow and resulted in the formation of a rod- or column-like structure (Fig. 1A). In the literature, structures of this kind are referred to as row-structures, Keller–Machin structures, or layered lamellar structures [29–37]. The lamellae are assembled into columns and are predominantly located layerwise perpendicularly to the extrusion axis (Fig. 1A and B), although regions with disorder in the arrangement of the lamellae are also observed.

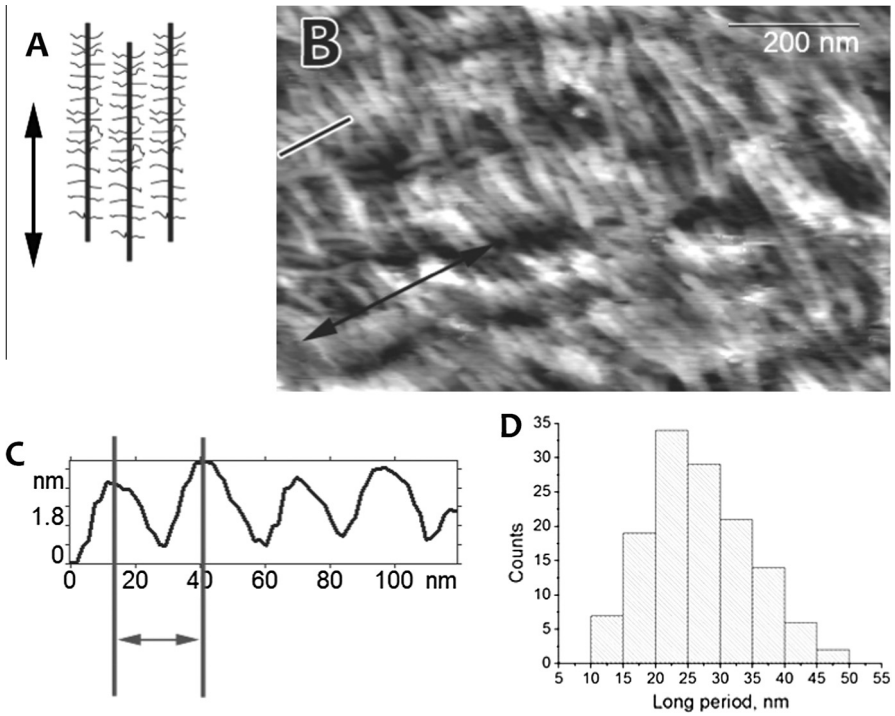

Fig. 1. (A) Schematic representation of the row-structure of a polymer produced by extrusion blow molding [33] and (B) AFM image of initial HDPE, with the line indicating the direction of the section profile (C) along the extrusion axis, the vertical lines in the profile denote the tops of lamellae, and the arrows in panels (A) and (B) indicate the extrusion axis. Panel (D) depicts the histogram of long period distribution for initial HDPE.

In order to perform the AFM examinations of the undeformed and deformed films under the same conditions, the structure of the initial samples was studied in the liquid medium. The AFM images were used to plot the profiles of sections along the extrusion axis (Fig. 1B). The distance between the maxima in the section profiles (Fig. 1C) corresponds to the distance between neighboring lamellae; i.e., represents the value of the long period.

The obtained data were used to plot the histogram of long period distribution (Fig. 1D). The mean value of the long period determined by AFM was 27 ± 8 nm. For HDPE under investigation, this value has appeared to be in good agreement with the results obtained by SAXS, according to which the long period amounts to 25 nm [48].

3.2. Peculiarities of HDPE deformation in the liquid medium by the crazing mechanism

Polymer deformation in liquid media by the crazing mechanism is distinguished by a decrease in tensile stress and an increase in polymer volume, as compared with the stretching in air [19]. Fig. 2 depicts the engineering stress–strain curves for stretching along the axis of HDPE extrusion in air (curve 1) and in water–ethanol solution (curve 2). It can be seen that, as compared with the stretching in air, the HDPE deformation in liquid medium is not accompanied by a change in the elasticity modulus of the polymer, and the tensile stress decreases in the region of the yield point.

Previous studies of crazing [19,20] have shown that the deformation of HDPE in contact with liquid plasticizers is accompanied by a reduction in the elasticity modulus and a noticeable decrease in the yield stress. The deformation of HDPE in liquids in which the polymer does not swell significantly (the degree of HDPE swelling in the water–ethanol medium is no higher than 1%) occurs without a reduction in the elasticity modulus but with a decrease in the tensile stress in the region of the yield point. Seemingly, the influence of these media is, to a greater extent, associated with a reduction in the interphase surface energy; i.e., the water–ethanol solution selected for the work turns out to be an adsorption-active medium for HDPE.

As can be seen from the comparison between the stress–strain curves measured for the deformation along (Fig. 2, curves 1, 2) and perpendicularly (Fig. 2, curves 3, 4) to the extrusion axis, the direction of the stretching force with respect to the extrusion axis is of importance for HDPE films, which have a pronounced anisotropic layered structure. HDPE is deformed in the direction of the extrusion axis at a higher stress, although it may be related to the fact that the engineering stress–strain curves do not take into account variations in the cross-sectional areas of the samples upon stretching.

Since crazing is accompanied by the formation of a highly disperse fibrillar–porous structure, volume increment is an important characteristic for polymer deformation in liquid medium. The value of volume strain allows one to infer the stretching mechanism and the efficiency of crazing from the viewpoint of the formation of the nanoporous structure: the higher the volume strain the higher the efficiency of crazing.

The volume strain of HDPE samples is presented in Fig. 3 as function of tensile strain. It can be seen that deformation in air (curve 1) and stretching in the liquid medium in the direction perpendicular to the extrusion axis (curve 3) do not lead to the increasing the sample volume.

When HDPE is deformed in the direction coinciding with the extrusion axis, its volume strain initially (up to a tensile strain of 200%) dramatically increases; then, the volume strain actually does not grow in the entire range of tensile strains (curve 2) that is typical for semicrystalline polymers being deformed by the crazing mechanism.

Fig. 4 shows the photographs taken from samples, which were deformed, placed in a dye solution, washed in running water, and dried. It can be seen that the dye has only penetrated into the samples deformed in the liquid medium along the extrusion axis (Fig. 4A). Samples deformed in the liquid medium perpendicularly to the extrusion axis are slightly colored in their middle part

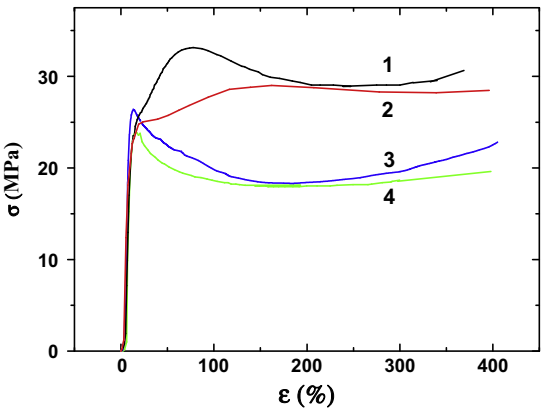

Fig. 2. Engineering stress–strain curves for HDPE films being deformed along the extrusion axis in (1) air and (2) in water–ethanol solution and perpendicularly to the extrusion axis in (3) air and (4) in water–ethanol solution.

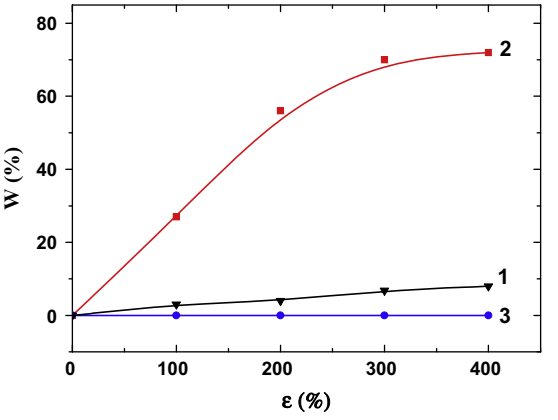

Fig. 3. Dependences of volume strain W on tensile strain ε of HDPE upon deformation (1, 2) along the extrusion axis in (1) air and (2) in water–ethanol solution; (3) perpendicularly to the extrusion axis in water–ethanol solution.

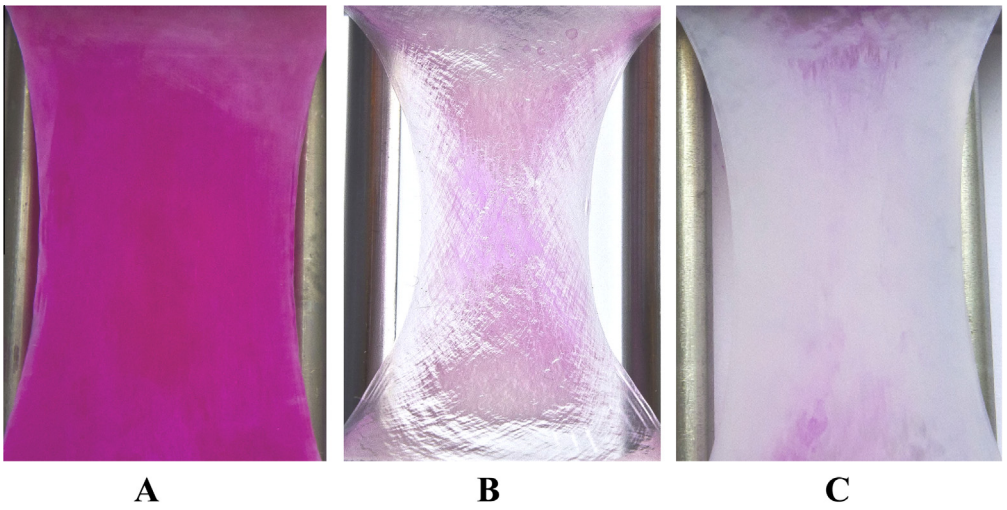

Fig. 4. Photographs of HDPE samples deformed by 200% in water–ethanol solution (A) along the extrusion axis and (B) perpendicularly to the extrusion axis, as well as (C) along the extrusion axis in air.

(Fig. 4B). It can be seen that the deformation is accompanied by the appearance of shear bands, and the dye penetrates namely into these local zones. These bands may be referred to as shear-crazes. Such formations have previously been observed [49]. However, deformation of this kind is not accompanied by a noticeable increase in sample volume, which is evident from the data on the volume strain of the deformed samples (Fig. 3, curve 3) and from the lateral contraction of the deformed films that is inherent in deformation through the shear mechanism. The samples deformed in air (Fig. 4C) open porous structure is not formed under these conditions.

The superposition of the data on the volume strain (Fig. 3) and the stress–strain curves (Fig. 2) with the structure of initial HDPE (Fig. 1) shows that the deformation occurs by the crazing mechanism when the direction of the stretching force is perpendicular to the planes in which the layers of lamellae lie. Moreover, the deformation by the crazing mechanism takes place only in the presence of the water–ethanol medium. It is known that cavitations (microvoids) that arise during deformation of semicrystalline polymers may either collapse or grow with an increase in the tensile strain. It is obvious that, in the presence of a physically active media, which reduces the interphase surface energy, the microvoids are stabilized and a porous structure permeable to liquids is developed [17–21]. The water–ethanol medium, which is adsorption-active for HDPE, fills and stabilizes the microvoids formed during deformation, thereby promoting the development of a network of interconnected pores permeable to the liquid throughout the bulk polymer. In the absence of the medium, the polymer is deformed with necking. Thus, if, at some stage of stretching in air, micropores are formed, they do not coalesce into a united permeable porous structure. So, the direction of an applied force and the presence of a physically active media are the key factors for the development of deformation of HDPE with an initial row-structure by the crazing mechanism.

3.3. AFM study of the structural evolution of HDPE deformed in the liquid medium by the crazing mechanism

Let us consider the evolution of the structure of HDPE during stretching along the extrusion axis in the water–ethanol medium, i.e., under the conditions providing the deformation through the crazing mechanism. The AFM images presented in Figs. 5–8 were taken from samples stretched to different tensile strains. At each tensile strain, the distribution histograms were plotted based on the AFM data, and the following parameters were determined: the mean value of the long period, i.e., the distance between the lamellae or the distance between the maxima in the section profiles along the stretching axis, and the mean lamella thickness, which was determined as the half-width

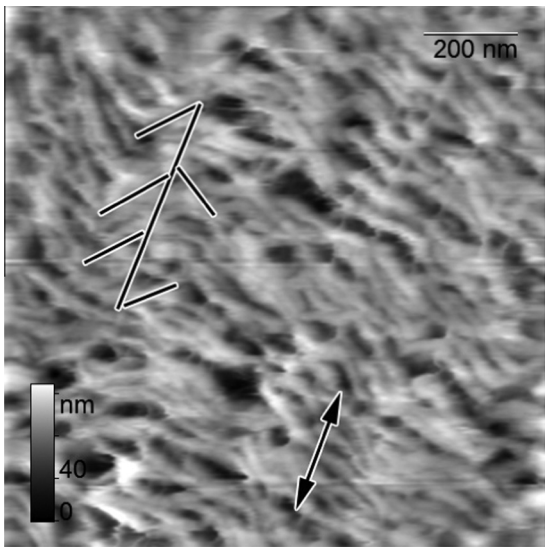

Fig. 5. AFM image of HDPE deformed in water–ethanol solution by 50% along the extrusion axis (indicated by arrow).

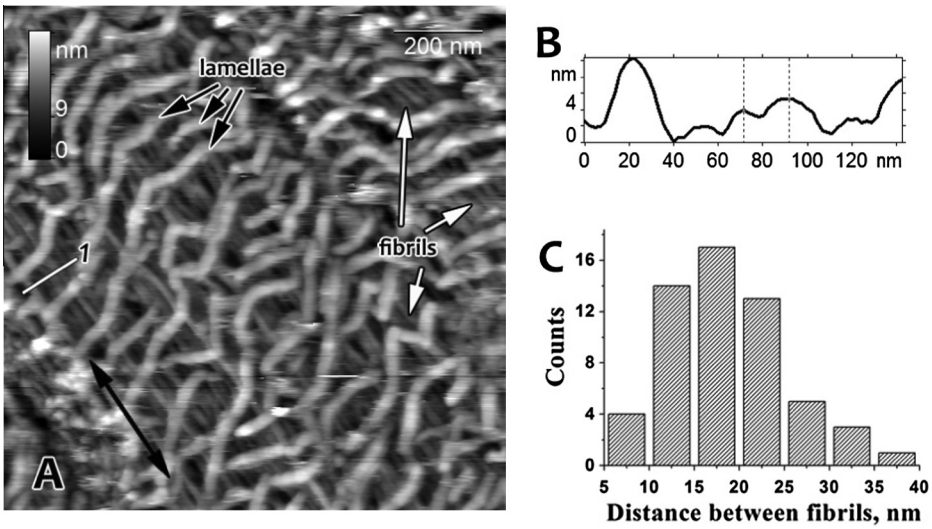

Fig. 6. (A) AFM image of HDPE stretched by 100% in water–ethanol solution. The stretching direction is denoted by the arrow. (B) Section profile constructed along line (1) in image (A), with the vertical dotted lines in the profile denoting the tops of fibrils. (C) Distribution histogram for the value representing the sum of the width of a slit (pore) between fibrils and the diameter of a fibril in deformed HDPE.

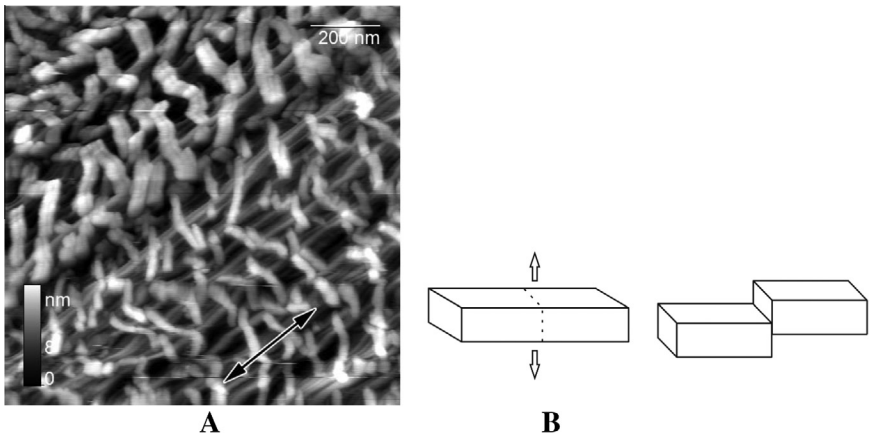

Fig. 7. (A) AFM image of HDPE stretched by 200% in water–ethanol solution. The direction of the stretching coincides with the extrusion axis and is denoted by the arrow. (B) Scheme of disruption of lamellae into fragments.

of a peak. For the undeformed sample the lamella thickness was measured from SAXS and DSC [48]. The obtained data are listed in Table 1.

As can be seen from the comparison between Figs. 1 and 5, deformation causes noticeable changes in the structure of initial HDPE. It is evident that, even at a tensile strain of 50%, the majority of lamellae are bent and located not perpendicularly to the stretching axis (extrusion axis) (as shown lines in Fig. 5). The values of the long period increase from 27 ± 8 nm for undeformed HDPE films to 40 ± 11 nm at a tensile strain of 50%. The thickness of lamellae is 16 ± 3 nm (Table 1), as determined from the section profiles.

The volume strain of the samples stretched by 50% is not higher than 15% (Fig. 3, curve 2), as measured from the geometric sizes of the samples, and no pronounced fibrillar–porous structure is observed at this tensile strain.

Fig. 6A exhibits the AFM image of the surface of an HDPE film stretched by 100% in water–ethanol solution. In the course of the deformation by 100%, the long period value varies in a wide range, and its mean value increases to 55 ± 17 nm, thereby indicating the separation of lamellae with the increase in the tensile strain. The thickness of lamellae is retained in the same range (the mean value is 17 ± 3 nm), and their bend remains preserved. The main change in the structure of HDPE consists in the appearance of a developed fibrillar–porous structure in the interlamellar space. Fibrils oriented along the stretching axis are distinctly seen between lamellae in the images of HDPE stretched by 100%. Slitlike pores are observed between the fibrils.

This image does not enable us to determine reliably the diameters of the fibrils and voids, because the cantilever curvature radius is nearly 10 nm, and the measurements

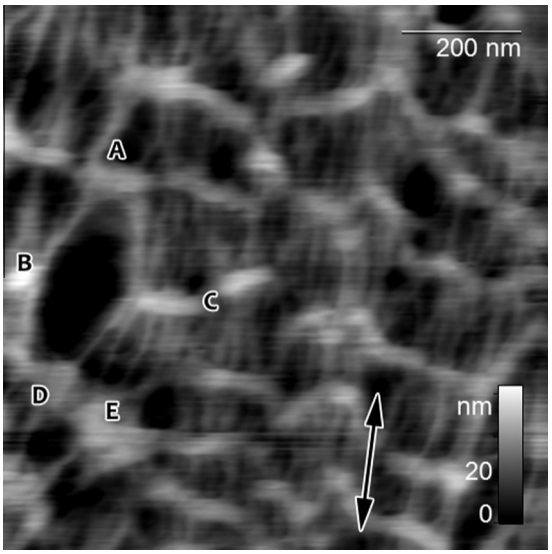

Fig. 8. AFM image of HDPE deformed by 400% in water–ethanol solution. The direction of the stretching is denoted by the arrow.

Table 1
Parameters (mean ± standard deviation) of the structure of HDPE as depending on tensile strain ε during crazing in liquid medium.

ε (%)	Long period (nm)	Lamella thickness (nm)	Pore width + fibril diameter (nm)
0	27 ± 8	14	–
50	40 ± 11	16 ± 3	–
70	48 ± 15	16 ± 3	–
100	55 ± 17	17 ± 3	19 ± 7
200	75 ± 36	16 ± 3	20 ± 6
400	128 ± 50	–	33 ± 13

of the surface asperities having sizes comparable with this value are incorrect. The distance between the tops of fibrils is independent of the cantilever curvature radius; therefore, the value that represents the sum of the diameter of a fibril and the width of a slit (pore) between fibrils may be measured with a rather high accuracy. In order to measure this parameter, section profiles were plotted along the lines perpendicular to the stretching axis (along line 1 in Fig. 6A). The distance between the tops of fibrils was determined from the obtained section profiles. The results of measuring the value corresponding to sum of the width of a slit (pore) between fibrils and the diameter of a fibril are presented as a histogram in Fig. 6C. The mean value has appeared to be 19 ± 7 nm. This parameter may be estimated in another way. As can be seen from the profilogram and the obtained images, a segment 100 nm long contains, on average, five fibrils, so the value corresponding to sum of the diameter of one fibril and one pore is on the order of 20 nm.

Thus, the images obtained at a tensile strain of 100% obviously visualize the previous ideas of the development of a fibrillar–porous structure during the deformation of semicrystalline polymers by the crazing mechanism. Previously, these ideas were based on an increase in the volume of a polymer sample and the emergence of a structure permeable to liquids after the deformation of semicrystalline polymers in liquid medium, as well as on SAXS data [20,50].

Fig. 7A depicts the AFM image of an HDPE sample deformed in water–ethanol medium by 200%. It can be seen that, at this tensile strain, lamellae have been disrupted into smaller fragments (Fig. 7B). Even the largest fragments are no longer than 200 nm. It should also be noted that the fragments of lamellae are displaced relative to each other. The fragments of lamellae may be oriented at various angles to the direction of stretching. The thickness of lamellae (16 ± 3) nm remains in the same range.

The data presented in Table 1 demonstrate that the long period continues to grow with the tensile strain, and its values vary in wide range. The mean long period value is 75 ± 36 nm. The mean value of the sum of the fibril diameter and the pore width is 20 ± 6 nm; i.e., as compared with this value for HDPE stretched by 100% (19 ± 7 nm) (Table 1).

After stretching by 400%, the HDPE structure resembles a network of fibrils with nodes formed by the fragments of lamellae (Fig. 8). At this tensile strain, lamellae are disrupted into fragments 50–100 nm long, which are displaced relative to each other.

The fragmentation of lamellae and the displacement of their fragments substantially increase the parameter reflecting the sum of fibril diameter and pore width (the mean value is 33 ± 13 nm). As can be seen from Fig. 8, at this geometry of a sample fibrils "originating" from one lamella may "end" in two different fragments of a disrupted neighboring lamella. This circumstance facilitates the formation of large voids. The ends of fibrils originating from lamella fragment A are attached to separate fragments B and C, whereas fibrils originating from fragment C "come" to fragments D and E, which, most likely, composed one lamella before the fragmentation. Thus, as the tensile strain of HDPE is increased to 400%, the fragmentation of lamellae and the displacement of their fragments relative to each other become especially pronounced, while the values of the long period and the sum of the fibril thickness and pore width increase (Table 1).

As mentioned above, the AFM measurements do not make it possible to reliably determine the width of the slits (pores) between fibrils. However, assuming that, at a tensile strain of 100–200%, the thickness of a fibril is equal to the diameter of a pore, the "pore width + fibril diameter" values determined by AFM may be used to estimate the pore width (pore diameter) in HDPE as a value of about 6–13 nm at tensile strains of 100% and 200%, respectively. The similar fibril diameters and pore widths (about 8–10 nm) were also obtained by SAXS for crazed HDPE [51]. In work [52] the parameters of the fibrillar–porous structure of HDPE deformed by the crazing mechanism (that is used in this work) were determined by the pressure-driven liquid permeability method. The porous structure of the polymer was simulated by a system of straight channels running through the cross section of a film. The effective pore diameter was calculated by the Poiseuille equation. For HDPE deformed in different media by

100–200%, the effective pore diameter appeared to be 4–8 nm. Thus, different methods yield close values of pore diameters for HDPE deformed in liquid media by the crazing mechanism.

Images illustrating the structural rearrangements that accompany the stretching of HDPE in water–ethanol solution and the scheme constructed by summarizing the data are presented in Fig. 9.

The comparison of the AFM images (Fig. 9) with the data in Table 1 and the stress–strain curve for HDPE deformation in water–ethanol solution (Fig. 2) allows us to describe the process of HDPE deformation by the crazing mechanism as follows. At an initial stage of stretching (below the yield stress), the stress–strain dependence is linear. According to the published data [53], the deformation of crystalline polymers begins in the more compliant amorphous phase, this deformation being reversible owing to the rubberlike properties of through chains. Further, as the tensile strain increases, lamellae are bent (Figs. 5A, 9B) that agrees with the data on the deformation of semicrystalline polymers (in particular, so called hard-elastic polymers) in air [54]. The locking of the shear of

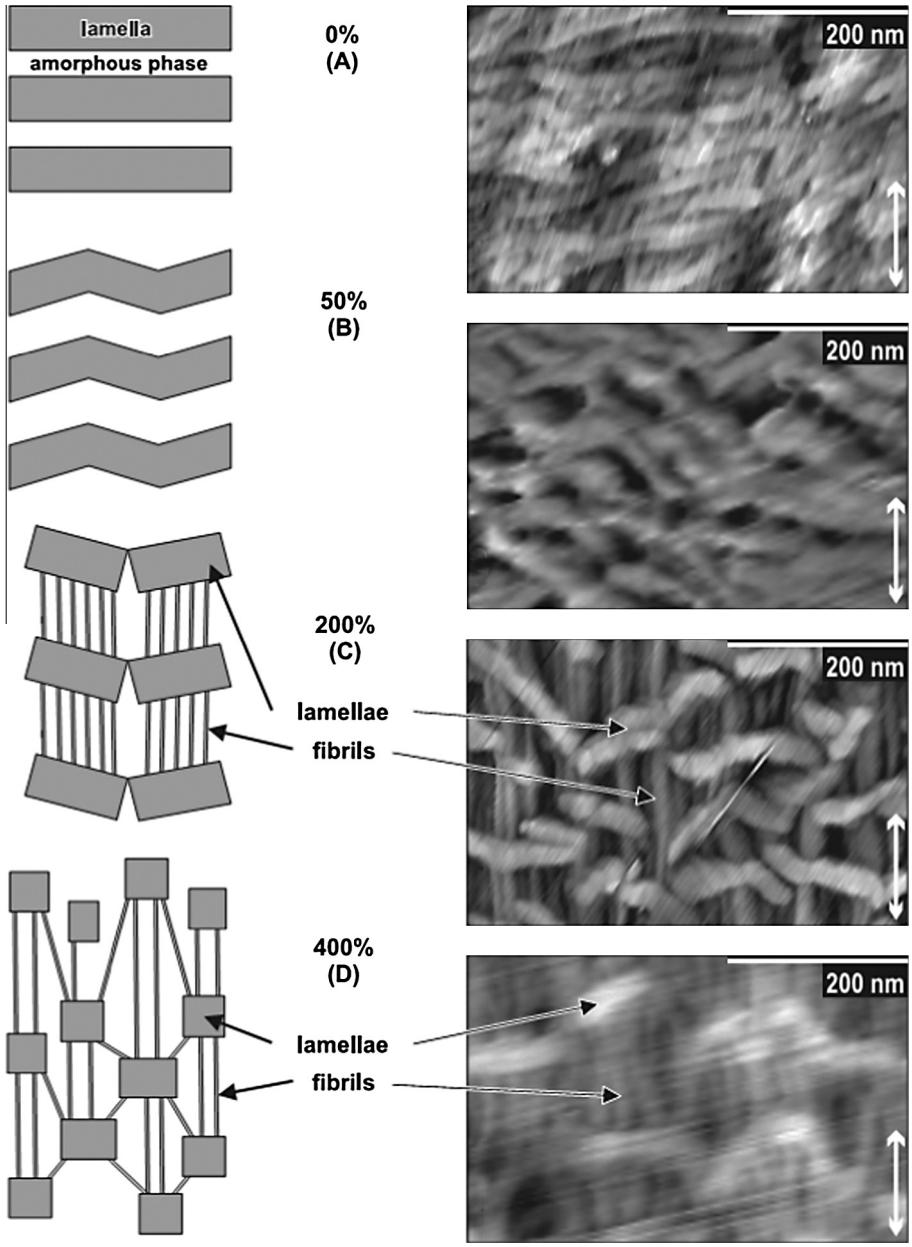

Fig. 9. AFM images of (A) initial HDPE and that stretched by (B) 50%, (C) 200%, and (D) 400% in water–ethanol solution. The stretching direction coincides with the extrusion axis and is denoted by the arrows in the images. The scheme constructed based on the images is shown in the left-hand part of the figure.

amorphous layers due to straining of tie-molecules causes stress concentrations in lamellae (at interfaces around points of tie-molecules entrance into lamella) and results in lamellae bending according to the crystallographic mechanisms [10].

In addition to the bending of lamellae, the growth of the long period, i.e., the separation of the lamellae, takes place. It is this stage at which, in the opinion of many authors [6,7,55,56], microvoids (cavitations) are nucleated. The separation of lamellae must be accompanied by either the development of cavitations in the amorphous component with the formation of crazes (voids) [6,7], or the plastic flow of the material toward the sites of defective packing of polymer chains [2].

The deformation resistance to the separation of lamellae depends on the densities of tie chains and entanglement network in the amorphous phase, as well as the thickness of lamellae [7,57]. The separation lamellae cannot continue at high tensile strains, because the tie chains in the amorphous phase can only be stretched to some limiting state [58–60]. The taut tie-molecules produce stress concentrations on lamellae surfaces, which together with crystallographic slip instabilities lead to slip localization. As a consequence, lamellae undergo splitting and fragmentation into blocks – the next stage of deformation [10,61].

The analysis of the images (Figs. 5–8) taken in the physically active medium from HDPE stretched to different tensile strains shows that the extent of lamella fragmentation increases with the tensile strain: at a tensile strain of 100%, extended fragments of lamellae (as long as 500 nm) are observed; at a tensile strain of 200%, the longitudinal sizes of lamellae decrease to 100–200 nm; and, at a tensile strain of 400%, this value becomes still smaller (nearly 50–100 nm). As can be seen from the obtained AFM images of HDPE stretched in the physically active medium, when passing from 50% to 100% tensile strain, substantial changes take place in the polymer structure, namely, fibrils and pores arise.

At present, there are several models for the transformation of a lamellar structure into a fibrillar one: the Peterlin's micronecking model [1,5], the melting–recrystallization model [62,63] and the crystallographic model [2,64–66]. Despite the variety of models the majority of researchers believe that the breakage of a crystal structure (the fragmentation of lamellae and the transformation of a lamellar structure into a fibrillar one) and the development of cavitations begin in the region of the yield stress, and this fact is confirmed by our data.

The data presented in Table 1 were used to plot the dependence of the mean long period values on the tensile strain (Fig. 10, curve 1), which appeared to be almost linear. Moreover, the plotted curve agreed with the theoretical straight line (Fig. 10, curve 2) constructed under the assumption that the deformation occurs entirely due to the separation of lamellae in accordance with the following equation: $L = L_0(1 + \varepsilon)$, where L is the long period value calculated at tensile strain ε and L_0 is the long period value for the initial polymer. Taking into account that the lamella thickness remains unchanged within the measurement error, this fact leads us to state that deformation of HDPE

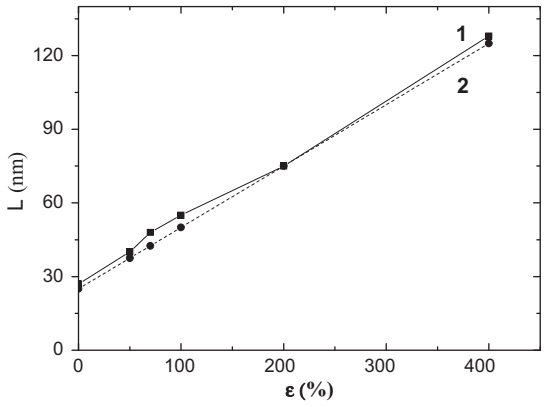

Fig. 10. Dependences of the mean long period values of HDPE on the tensile strain upon stretching in water–ethanol solution according to the AFM data (solid line 1) and calculations (dotted line 2).

with the initial row-structure in the physically active medium proceeds via the separation of lamellae. An analogous coincidence between the calculated values of the long period and SEM data was observed for hard-elastic polymers deformed in air [67].

The AFM data exhibit the similarity of the structure and behavior of semicrystalline polymers upon crazing in liquid medium and hard-elastic polymers deformed in air [68–70]. This similarity is not accidental, since it is based on the layered lamellar structure (row-structure), which is common for these groups of polymers. Owing to the special procedures applied for stretching and annealing, the structure of precursor films used for producing hard-elastic polymers is more perfect; therefore, a fibrillar–porous structure with a high porosity is formed in them even upon stretching the polymers in air.

3.4. HDPE deformation in the liquid medium upon stretching in the direction perpendicular to the extrusion axis

As has been mentioned above, the planes of lamellae are mostly oriented perpendicularly to the extrusion axis, and the studies have been performed with samples deformed along the extrusion axis (normal to the lamellae planes). In this case the deformation by crazing takes place. In order to find out the effects of the initial arrangement of lamellae and the direction of the applied force on the resulting structure, we studied HDPE deformed in water–ethanol solution by 200% in the direction perpendicular to the extrusion axis (Fig. 11A and B). It has been shown above (Fig. 3, curve 3) that, in this case, the volume of the polymer does not increase upon deformation, and the dye does not color a sample (Fig. 4B); i.e., the crazing mechanism is not realized.

It can be seen that deformation is accompanied by the appearance of many thick (15–40 nm) strands, which resemble the lamellae shifted relative to each other (Fig. 11A and B). According to [66] this deformation mechanism involves the shear of the lamella crystals parallel to each other (scheme in Fig. 11C). Some images of the initial film show regions where the lamella

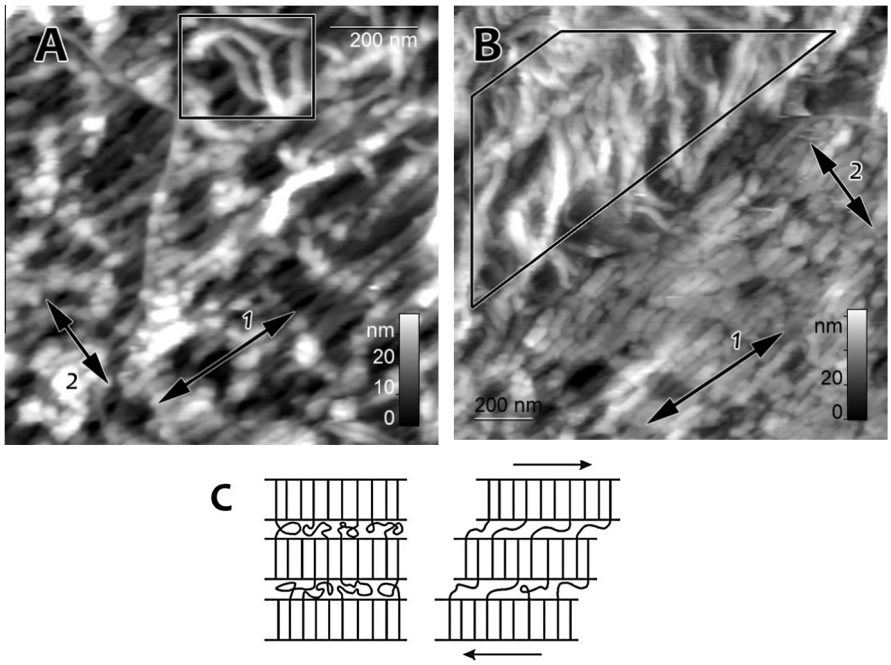

Fig. 11. (A and B) AFM image of HDPE deformed in water–ethanol solution by 200% in the direction perpendicular to the extrusion axis (arrow 1 denotes the stretching direction, arrow 2 denotes the extrusion axis) and (C) scheme of the slip (shear) of lamellae under the conditions when the stress is applied perpendicularly to the normal to the plane of lamella surfaces [66].

arrangement is disturbed and the planes of lamellae are not oriented perpendicularly to the extrusion axis but rather at an angle to it or along it. Apparently, the deformation of such regions leads to the lamellae oriented perpendicularly or at an angle to the stretching direction (as shown in the marked areas in Fig. 11A and B).

Thus, the mechanism of deformation – crazing with the separation of lamellae and the formation of the fibrillar–porous structure or the slip (shear) of lamellae relative to each other (Fig. 11C) with no pore formation – depends on the direction of the deforming force with respect to the arrangement of lamellae in the initial HDPE structure. The deformation in the direction perpendicular to the extrusion axis is not accompanied by the development of voids; therefore, the absence of crazing is quite an expected result.

3.5. The features of crazing amorphous glassy and crystalline polymers

Crazing is a type of plastic deformation of polymers, which is, in contrast to shear, accompanied by an increase in the volume of a sample being deformed [71]. Previously, the mechanism of crazing and the conditions of the transition from the crazing to the shear were mainly considered for amorphous glassy polymers at deformation temperatures below the glass-transition temperatures of the polymers [17,72,73]. The deformation develops in some distinctly distinguishable local zones (crazes). The data on the structure of crazes were, for the first time, reported in the works by Kambour [17]. At present, a model craze structure has been recognized, which implies the existence of "main" fibrils that connect the opposite walls of crazes and transverse fibrils between them [74].

Deformation of semicrystalline polymers may also be accompanied by the development of crazes analogous to crazes in amorphous glassy polymers [75–77]. The growth of crazes and the development of deformation by the mechanism of crazing rather than shear depend primarily on the density of the effective entanglement network and the surface energy of a polymer irrespective of whether the polymer is amorphous or semicrystalline [78]. The transition of deformation from the shear to crazing is facilitated by a reduction in the surface energy of a polymer, which may be realized when stretching polymers in physically active media [17,19,72,73].

However, the behavior of semicrystalline polymers in the course of crazing is distinguished by some specific features. As a matter of fact, two types of crazing may be observed for semicrystalline polymers. The "classical" crazing, which is similar to the crazing of amorphous glassy polymers, takes place when a semicrystalline polymer is deformed at a temperature in the vicinity or below the glass-transition temperature of its amorphous phase.

When a semicrystalline polymer is stretched at a temperature above the glass-transition temperature of its amorphous phase, the deformation may also lead to the nucleation of cavitations in the interlamellar region [6,7], and their subsequent development may be accompanied by the development of crazes characterized by a typical fibrillar–porous structure [75–77]. This type of crazing may be referred to as "intercrystallite" or "interlamellar" crazing.

Two types of crazing may be observed when deforming semicrystalline polymers in physically active media, which facilitate the development of deformation by the crazing mechanism. In this case, the type of crazing, through which the deformation occurs, depends on the deformation conditions (temperature and rate of deformation), the degree of polymer crystallinity, and the nature of a physically active liquid (adsorption-active medium or liquid, in which the polymer swells). In the literature [20] the difference between the classical and interlamellar (the authors refer to the latter as "delocalized" crazing) types of crazing was considered upon deformation of polymers in physically active liquid media. The width of crazes resulting from the classical crazing may be as large as several dozen micrometers, while their length may be still larger, i.e., a few millimeters and above. The development of the classical crazing of this type is associated with an initial imperfection of a material, while individual crazes, as well as regions of an undeformed polymer between them, may be distinguished in a sample. As the deformation develops, the fraction of the nonoriented bulk polymer between crazes continuously diminishes until the entire polymer passes into the oriented state [19].

At present, the evolution of the structure of amorphous glassy polymers deformed by the classical crazing mechanism has been studied in detail, whereas the structural aspects of the interlamellar crazing remain to be investigated. In connection to all of the mentioned above, this work represents the first direct investigation of the structural evolution of a semicrystalline polymer deformed by the interlamellar crazing.

As has been shown in this work, crazes in HDPE deformed by the interlamellar crazing are located between lamellae or stacks of lamellae and have a size of no larger than 200 nm even at high tensile strains. The nucleation and development of crazes in semicrystalline polymers are predetermined by their lamellar structure, and the developing fibrillar–porous structure is distributed in the intercrystallite space throughout the sample volume. Hence, the main difference between the two kinds of crazing consists in the sizes of the local zones of deformation.

4. Conclusion

Thus, the AFM study has demonstrated that deformation of HDPE having an initial row-structure by the interlamellar crazing is accompanied by the following processes: lamellar bending, separation of lamellae, disruption of lamellae into smaller fragments, the displacement of the fragments of lamellae relative to each other, and the formation of fibrillar–porous structure in the interlamellar space.

It was found that the long period increases in the proportion to the tensile strain. This fact indicates that the separation of lamellae makes the main contribution to the deformation of HDPE by crazing mechanism. The fibrillar–porous structure develops in the case of stretching along the extrusion axis (perpendicular to the planes of the lamellae) and does not develop in the case of stretching in the transverse direction. The obtained data enable to determine the main difference between the classical and interlamellar crazing: the sizes of the local zones of deformation. The width of crazes resulting from the classical crazing may be as large as several dozen micrometers, while the width of crazes resulting from the interlamellar crazing does not exceed a few hundred nanometers.

Acknowledgements

This work was supported by the Russian Foundation for Basic Research. Project No. 15-03-03430-a, by the Grant of the State Support of the Leading Scientific Schools NSh-1683.2014.3. The work was partly performed at User Facilities Center of M.V. Lomonosov Moscow State University under financial support of Ministry of Education and Science of Russian Federation.

References

[1] Peterlin A. J Mater Sci 1971;6(6):490–508.
[2] Lin L, Argon AS. J Mater Sci 1994;29(2):294–323.
[3] Oleinik EF. Polym Sci Ser C 2003;45:17–117.
[4] Patlazhan S, Remond Y. J Mater Sci 2012;47(19):6749–67.
[5] Peterlin A. Colloid Polym Sci 1987;265(5):357–82.
[6] Galeski A. Prog Polym Sci 2003;28(12):1643–99.
[7] Pawlak A, Galeski A, Rozanski A. Prog Polym Sci 2014;39(5):921–58.
[8] Geil PH, Ginzburg BM. J Macromol Sci Part B: Phys 2006;45(2):291–323.
[9] Friedrich K. Adv Polym Sci 1983;52(53):225–74.
[10] Bartczak Z, Galeski A. Macromol Symp 2010;294(1):67–90.
[11] Robeson LM. Polym Eng Sci 2013;53(3):453–67.
[12] Cazenave J, Seguela R, Sixou B, Germain Y. Polymer 2006;47(11):3904–14.
[13] Kurelec L, Teeuwen M, Schoffeleers H, Deblieck R. Polymer 2005;46(17):6369–79.
[14] Lagaron JM, Dixon NM, Reed W, Pastor JM, Kip BJ. Polymer 1999;40(10):2569–86.
[15] Lagaron JM, Pastor JM, Kip BJ. Polymer 1999;40(7):1629–36.
[16] Lagaron JM, Dixon NM, Gerrard DL, Reed W, Kip BJ. Macromolecules 1998;31(17):5845–52.
[17] Kambour RP. J Polym Sci Macromol Rev 1973;7(1):1–154.
[18] Kramer EJ. Developments in polymer fracture. London: Appl Sci; 1979.
[19] Volynskii AL, Bakeev NF. Solvent crazing of polymers. Amsterdam, New York, and Tokyo: Elsevier; 1995.
[20] Volynskii AL, Arzhakova OV, Yarysheva LM, Bakeev NF. Polym Sci Ser B 2000;42(3):549–64.
[21] Yarysheva LM, Volynskii AL, Bakeev NF. Polym Sci Ser B 1993;35:913–21.
[22] Bakeev NP, Lukovkin GM, Marcus I, Mikouchev AE, Shitov AN, Vanissum EB, et al. Imbibitions process. Patent US; 1996.
[23] Yarysheva AY, Bagrov DV, Rukhlya EG, Yarysheva LM, Volynskii AL, Bakeev NF. Polym Sci Ser A 2012;54(10):779–86.
[24] Trofimchuk ES, Nikonorova NI, Chagarovskii AO, Volynskii AL, Bakeev NF. J Phys Chem B 2005;109(34):16278–83.
[25] Yarysheva LM, Volynskii AL, Bakeev NF. Polym Sci Ser A 1997;39(1):26–42.
[26] Toncelli C, Arzhakova OV, Dolgova A, Volynskii AL, Bakeev NF, Kerry JP, et al. Anal Chem 2014;86(3):1917–23.
[27] Rukhlya EG, Litmanovich EA, Dolinnyi AI, Yarysheva LM, Volynskii AL, Bakeev NF. Macromolecules 2011;44(13):5262–7.
[28] Weichold O, Goel P, Lehmann K-H, Möller M. J Appl Polym Sci 2009;112(5):2634–40.
[29] Keller A, Machin MJ. J Macromol Sci Part B: Phys 1967;1(1):41–91.
[30] Yu T-H, Wilkes GL. Polymer 1996;37(21):4675–87.
[31] Zhou H, Wilkes GL. Polymer 1997;38(23):5735–47.
[32] Kojima M, Magill JH, Lin JS, Magonov SN. Chem Mater 1997;9(5):1145–53.
[33] Zhang XM, Elkoun S, Ajji A, Huneault MA. Polymer 2004;45(1):217–29.
[34] Godshall D, Wilkes G, Krishnaswamy RK, Sukhadia AM. Polymer 2003;44(18):5397–406.
[35] Prasad A, Shroff R, Rane S, Beaucage G. Polymer 2001;42(7):3103–13.

[36] Lu J, Sue HJ, Rieker TP. Polymer 2001;42(10):4635–46.
[37] Yu T-H, Wilkes GL. Polymer 1997;38:1503–5.
[38] Butler MF, Donald AM, Ryan AJ. Polymer 1998;39(1):39–52.
[39] Che J, Locker CR, Lee S, Rutledge GC, Hsiao BS, Tsou AH. Macromolecules 2013;46(13):5279–89.
[40] Li H, Zhou W, Ji Y, Hong Z, Miao B, Li X, et al. Polymer 2013;54(2):972–9.
[41] Nikolaeva GY, Prokhorov KA, Pashinin PP, Gordeyev SA. Laser Phys 1999;9(4):955–8.
[42] Opdahl A, Somorjai GA. J Polym Sci Part B: Polym Phys 2001;39(19):2263–74.
[43] Li DS, Garmestani H, Alamo RG, Kalidindi SR. Polymer 2003;44(18):5355–67.
[44] Brady J, Thomas E. J Mater Sci 1989;24(9):3311–8.
[45] Butler MF, Donald AM. J Mater Sci 1997;32(14):3675–85.
[46] Adams WW, Yang D, Thomas E. J Mater Sci 1986;21(7):2239–53.
[47] Michler GH. Colloid Polym Sci 1992;270(7):627–38.
[48] Bagrov DV, Yarysheva AY, Rukhlya EG, Yarysheva LM, Volynskii AL, Bakeev NF. J Microsc 2014;253(2):151–60.
[49] Li JCM. Polym Eng Sci 1984;24(10):750–60.
[50] Sinevich EA, Bykova IV, Bakeev NF. Polym Sci Ser A 1998;40(10):1671–80.
[51] Yefimov AV, Sherba VY, Ozerin AN, Rebrov AV, Bakeev NF. Polym Sci Ser A 1990;32(4):828–34.
[52] Arzhakova OV, Dolgova AA, Yarysheva LM, Volynskii AL, Bakeev NF. Inorg Mater: Appl Res 2011;2(5):493–8.
[53] Truss RW, Clarke PL, Duckett RA, Ward IM. J Polym Sci Polym Phys Ed 1984;22(2):191–209.
[54] Garber CA, Clark ES. J Macromol Sci Part B: Phys 1970;4(3):499–517.
[55] Humbert S, Lame O, Chenal JM, Rochas C, Vigier G. Macromolecules 2010;43(17):7212–21.
[56] Zhang XC, Butler MF, Cameron RE. Polymer 2000;41(10):3797–807.
[57] Lustiger A, Markham RL. Polymer 1983;24(12):1647–54.
[58] Lee BJ, Parks DM, Ahzi S. J Mech Phys Solids 1993;41(10):1651–87.
[59] Lee BJ, Argon AS, Parks DM, Ahzi S, Bartczak Z. Polymer 1993;34(17):3555–75.
[60] Parks DM, Ahzi S. J Mech Phys Solids 1990;38(5):701–24.
[61] Seguela R, Gaucher-Miri V, Elkoun S. J Mater Sci 1998;33(5):1273–9.
[62] Flory PJ, Yoon DY. Nature 1978;272:226–9.
[63] Gent AN, Madan S. J Polym Sci Part B: Polym Phys 1989;27:1529–42.
[64] Seguela R. J Polym Sci Part B: Polym Phys 2002;40:593–601.
[65] Galeski A, Bartczak Z, Argon AS, Cohen RE. Macromolecules 1992;25:5705–18.
[66] Bowden PB, Young Rd. J Mater Sci 1974;9(12):2034–51.
[67] Hild S, Gutmannsbauer W, Lüthi R, Fuhrmann J, Güntherodt HJ. J Polym Sci Part B: Polym Phys 1996;34(12):1953–9.
[68] Sprague BS. J Macromol Sci Part B: Phys 1973;8(1–2):157–87.
[69] Cannon SL, McKenna GB, Statton WO. J Polym Sci Macromol Rev 1976;11(1):209–75.
[70] Volynskii AL, Yarysheva AY, Rukhlya EG, Efimov AV, Yarysheva LM, Bakeev NF. Russ Chem Rev 2013;82(10):988.
[71] Kausch HH. Polymer fracture. New York: Springer-Verlag; 1987.
[72] Kramer E. Adv Polym Sci 1983;52(53):1–56.
[73] Kramer E, Berger L. Adv Polym Sci 1990;91(92):1–68.
[74] Brown HR. Macromolecules 1991;24(10):2752–6.
[75] Plummer CJG, Goldberg A, Ghanem A. Polymer 2001;42(23):9551–64.
[76] Thomas C, Ferreiro V, Coulon G, Seguela R. Polymer 2007;48(20):6041–8.
[77] Plummer CJG, Cudré-Mauroux N, Kausch HH. Polym Eng Sci 1994;34(4):318–29.
[78] Deblieck RAC, van Beek DJM, Remerie K, Ward IM. Polymer 2011;52(14):2979–90.